Mixing in Liquid-Jet-Agitated Tanks: Effects of Jet Asymmetry

ARTICLE *in* INDUSTRIAL & ENGINEERING CHEMISTRY RESEARCH · JANUARY 2005

Impact Factor: 2.59 · DOI: 10.1021/ie0496683

Mixing in Liquid-Jet-Agitated Tanks: Effects of Jet Asymmetry

Habib D. Zughbi* and Iqtedar Ahmad

Department of Chemical Engineering, King Fahd University of Petroleum & Minerals, Box 124, Dhahran 31261, Saudi Arabia

Mixing in liquid-jet-agitated tanks has been studied experimentally and numerically. A bottom-pump-around tank with a symmetric jet and another with an asymmetric jet arrangement were used. Conductivity was experimentally measured to determine the time required to achieve 95% mixing. Good agreement was obtained between the experimental and numerical results over a wide range of jet Reynolds numbers. Mixing time was found to be a function of the jet Reynolds number. A comparison of experimental and simulation results for bottom-pump-around and side-pump-around tank geometries, both having a symmetric jet, showed that, for jet Reynolds numbers, N_{Rej}, less than 25 000, the side-pump-around tank geometry required less time to achieve 95% mixing. For N_{Rej} greater than 25 000, the mixing times for the two arrangements were nearly the same. The up-angle is defined as the angle the jet makes with a horizontal plane parallel to the bottom of the tank. This angle has a significant influence on the 95% mixing time. The 95% mixing time for an up-angle of 20° is found to be about 50% of the 95% mixing time for an up-angle of 45°. The asymmetry of the jet was found to reduce the mixing time. The 95% mixing time when an asymmetric jet was used was found to be up to 34% less than that when a symmetric jet was used.

Introduction

Mixing is an important unit operation in many chemical engineering applications. Mixing applications include the homogenization of components and various physical properties; emulsification; prevention of stratification; and improvements in the rate of heat transfer, mass transfer, and chemical reactions. Mixing can be achieved using stirred vessels, static mixers, liquid-jet-agitated tanks, or pipelines with tees. In this paper, mixing by liquid jet agitation is of interest. Jet mixers have several advantages over conventional mechanically agitated mixers. Less structural work is required to support the mixing jet. This results in capital cost reduction. Maintenance costs are also lower, as the maintenance of a jet mixing system is easier than that of a mechanically stirred system. The pump can be remote from the tank. In some cases, the same pump that is used to fill or empty the tank can be used to power the jet. Another advantage of a jet mixer is that it can be fitted into an existing tank. This might become necessary if mixing in an existing tank becomes insufficient because of a change of feed or design shortcomings. Jet mixing systems are more appealing for mixing processes involving chemically sensitive liquids, e.g., preparation of foodstuffs[1] and acids mixing.[2] Jet mixers are used for the homogenization of hydrocarbon and LNG storage tanks,[2] blending of an inhibitor into a monomer storage tank,[3] prevention of stratification, prevention of deposition of suspended particles, and mixing of reactant streams.

Fossett and Prosser,[4] who first introduced the idea of liquid jet mixers, used an inclined side-entry jet in a flat-base cylindrical tank. This jet was inclined at 45° to the tank base. The liquid depth in the tank was two-thirds of the tank diameter. Fox and Gex[5] investigated the blending of liquids in a jet-agitated tank. Coldrey[6] presented the idea of using a bottom-side-entering jet inclined at 45°, in a flat-base cylindrical tank with the liquid height equal to the tank diameter. Lane[1] supported the Coldrey design by arguing that the greater jet length allows the jet to have a much larger entrainment capacity and hence a greater mixing ability. Maruyama[7] supported the concept of the greatest jet length for effective liquid jet agitation in a flat-base cylindrical tank. The same argument was advanced by Harnby et al.[2] in their textbook on mixing. However, after about two decades of the Coldrey design, Zughbi and Rakib[8] reported an optimum angle of 30° for the bottom-side-entering inclined liquid jet, instead of the previously quoted 45°, for mixing in a flat-base cylindrical tank that had an aspect ratio (liquid height/tank diameter) of 1. The concept of the longest jet gives the lowest mixing time might still be true; however, the question is which injection angle gives the greatest jet length. When injected at an angle of 45°, a jet might dissipate before hitting the opposite wall. A different injection angle might help the jet to hit and connect to the opposite wall. This, in effect, gives a greater jet length and therefore could explain the findings of Zughbi and Rakib.[8]

Lane and Rice,[9−11] Maruyama et al.,[12] and Gosman and Simitovic[13] investigated mixing in a jet-agitated tank. Perona et al.[14] investigated mixing in large horizontal tanks agitated by fluid jets. Compared to extensive experimental work, only a limited literature is available on computational fluid dynamics (CFD) studies of mixing in fluid-jet-agitated tanks. These CFD studies include works by Jayanti,[15] Zughbi and Rakib,[8,16] and Patwardhan.[3]

In the previous experimental or numerical investigations of mixing, one or more symmetric jets were used. The mixing time in a jet-agitated vessel depends on the dead or low-velocity zones. If these zones are minimized or eliminated by some means, the mixing time is reduced. Accordingly, an asymmetric jet was introduced

* To whom correspondence should be addressed. E-mail: hdzughbi@kfupm.edu.sa.

10.1021/ie0496683 CCC: $30.25
Published on Web 01/25/2005

to investigate its effect on the mixing time. This asymmetric jet is discussed in the following sections.

Previous researchers suggested a number of correlations to calculate the mixing time. Fosset and Prosser[4] recommended a correlation that included only terms for the tank diameter, jet diameter, and jet velocity. Okita and Oyama[21] and Van de Vusse[22] proposed similar correlations independent of the jet Reynolds number. Fox and Gex[5] proposed a correlation containing the jet Reynolds number to calculate the mixing time. Lane and Rice[9,10] proposed a correlation containing the jet Reynolds number. It should be noted that, if these correlations are applied to the same system, such as the one considered in the present study, the values of mixing times obtained are not very different.

In the present study, the mixing time is measured for varying jet velocity. Results could be presented as mixing time versus jet velocity. However, presenting the results as mixing time versus the jet Reynolds number is more illuminating, because a jet velocity of, say, 0.5 m/s might not give a clear indication of the nature of the flow inside the tank. In a previous study, Zughbi and Rakib[8] varied the physical properties of the liquid as well and plotted their results as a function of Reynolds number.

Criteria for Liquid Jet Mixing

Two main criteria are available in the literature to quantify mixing. Some researchers[11,14,17,18] have based their studies on 99% mixing. However, in most experimental studies,[1−3,8,14] mixing time is measured as the time from the tracer addition to the time when 95% mixing is achieved. Mathematically, this time is given by the expression

$$\left|\frac{C-\bar{C}}{\bar{C}}\right| = m \tag{1}$$

where C is the concentration of the tracer anywhere in the mixing vessel and $\bar{C}$ is the expected final mean tracer concentration. When complete homogeneity is achieved, m is equal to 0. Thus, for 95% mixing, m is equal to 0.05. This relationship implies that the initial value of C before the addition of the tracer is zero. The tracer is usually an electrolyte solution, and its concentration is measured in terms of conductivity. The criterion given by eq 1 is used in the experimental work carried out in this study to calculate mixing time by using the conductivity technique.

If the measured variable is temperature, as in the simulation part of this study, a certain volume of the tracer at high temperature is patched with the bulk or main liquid in the mixing tank. The temperatures of both the tracer and the bulk liquid are known. Thus, the final mean value of temperature, $\bar{T}$, can be calculated. The physical properties of the tracer are the same as those of the bulk liquid, so there is no need to take into account the temperature dependency of the physical properties of both the tracer and bulk liquid. The 95% mixing is reached when the temperature anywhere inside the tank is within the range of $[\bar{T} \pm (\bar{T} - T) \times 0.05]$, where T is the initial temperature of the bulk liquid in the mixing tank. It should be noted that hot water is used as a massless tracer in the present simulations. This technique was previously used successfully.[6,8] The volume of the hot water is a few percent of the total volume of the tank and is placed just below the top surface of the tank halfway between the side walls.

Governing Equations

The governing equations for a general mixing problem are the mass, momentum, and energy equations. These are given below for a constant-density and -viscosity system after elimination of the appropriate terms.

The conservation of mass equation is

$$\frac{\partial v_x}{\partial x} + \frac{\partial v_y}{\partial y} + \frac{\partial v_z}{\partial z} = 0 \tag{2}$$

The equation of conservation of momentum in the x direction is

$$\rho\left(\frac{\partial v_x}{\partial t} + v_x\frac{\partial v_x}{\partial x} + v_y\frac{\partial v_x}{\partial y} + v_z\frac{\partial v_x}{\partial z}\right) = -\frac{\partial P}{\partial x} + \mu\left[\left(\frac{\partial^2 v_x}{\partial x^2} + \frac{\partial^2 v_x}{\partial y^2} + \frac{\partial^2 v_x}{\partial z^2}\right)\right] \tag{3}$$

The conservation of momentum in the y direction is

$$\rho\left(\frac{\partial v_y}{\partial t} + v_x\frac{\partial v_y}{\partial x} + v_y\frac{\partial v_y}{\partial y} + v_z\frac{\partial v_y}{\partial z}\right) = -\frac{\partial P}{\partial y} + \mu\left[\left(\frac{\partial^2 v_y}{\partial x^2} + \frac{\partial^2 v_y}{\partial y^2} + \frac{\partial^2 v_y}{\partial z^2}\right)\right] \tag{4}$$

The conservation of momentum in the z direction is

$$\rho\left(\frac{\partial v_z}{\partial t} + v_x\frac{\partial v_z}{\partial x} + v_y\frac{\partial v_z}{\partial y} + v_z\frac{\partial v_z}{\partial z}\right) = -\frac{\partial P}{\partial z} + \mu\left[\left(\frac{\partial^2 v_z}{\partial x^2} + \frac{\partial^2 v_z}{\partial y^2} + \frac{\partial^2 v_z}{\partial z^2}\right)\right] \tag{5}$$

The conservation of energy is

$$\rho C_p\left(\frac{\partial T}{\partial t} + v_x\frac{\partial T}{\partial x} + v_y\frac{\partial T}{\partial y} + v_z\frac{\partial T}{\partial z}\right) = k\left(\frac{\partial^2 T}{\partial x^2} + \frac{\partial^2 T}{\partial y^2} + \frac{\partial^2 T}{\partial z^2}\right) + 2\mu\left[\left(\frac{\partial v_x}{\partial x}\right)^2 + \left(\frac{\partial v_y}{\partial y}\right)^2 + \left(\frac{\partial v_z}{\partial z}\right)^2\right] + \mu\left[\left(\frac{\partial v_x}{\partial y} + \frac{\partial v_y}{\partial x}\right)^2 + \left(\frac{\partial v_x}{\partial z} + \frac{\partial v_z}{\partial x}\right)^2 + \left(\frac{\partial v_y}{\partial z} + \frac{\partial v_z}{\partial y}\right)^2\right] \tag{6}$$

Initial and Boundary Conditions

The initial conditions can be summarized as follows: The temperature of the bulk water is 27 °C, and the temperature of the tracer water is 80 °C. The initial bulk velocity is 0 m/s, and the tracer velocity is 0 m/s.

The boundary conditions used are summarized as follows: The heat flux at the walls is 0 W/m^2. The no-slip condition was assumed at all walls. As for the pump, it was represented by a momentum source, and different values (N/m^3) were specified in the negative-x direction to have certain jet velocities.

Solution Algorithms

The pressure, velocity, and temperature fields in a liquid-jet-agitated tank are resolved by solving the mass,

momentum, and energy conservation equations. These equations were solved using a general-purpose CFD package, FLUENT, version 6.0.12. Hot water was used as the tracer in this study. A volume of hot water was centrally placed just below the top of the tank. This volume was about 1.5% of the tank volume. The results are not dependent on the volume of the tracer, but a reasonable volume such as the one selected is required so that the final equilibrium value of the measured variable is clearly different from the initial value. It is important that the physical properties of the tracer do not change so that there is no effect on the results. Accordingly, the physical properties of water, namely, density, viscosity, and heat capacity, were taken as being constant in this study.

Two numerical models were developed to study the effects of geometry and flow asymmetry on mixing in the fluid liquid-jet-agitated tanks. The first model will be referred to as the symmetric jet model, because it involves a symmetric jet at an up-angle of 45°. In the second model, which will be referred to as the asymmetric jet model, an asymmetric jet with an up-angle of 45° and a side-angle of 15° is used. These tank geometries are similar to those used in the experimental work.

An unstructured tetrahedral mesh was used. The finite-volume method (FVM) is used by FLUENT for discretization of the Reynolds-averaged transport equations. The standard $k-\epsilon$ model was used in most of the current simulations.

Experimental Work

Two geometries are used in this paper. The first is a bottom-pump-around geometry as shown in Figure 1a. The second is a side-pump-around geometry as shown in Figure 1b. Two angles, an up-angle and a side-angle, are also frequently referred to in this paper. The up-angle is the angle that the jet makes with the tank bottom as shown in Figure 2a. The side-angle, shown in Figure 2b, is the angle that the jet makes with a normal central plane passing through the recycle suction. The bottom-pump-around tank geometry is more commonly used in industry. Mixing in such a geometry has not previously been investigated, either experimentally or numerically. Lane[1] and Lane and Rice[10] experimentally investigated mixing in a side-pump-around tank geometry involving a symmetric jet at an up-angle of 45°. Zughbi and Rakib[16] investigated mixing in this side-pump-around geometry numerically. The recycle suction point at the top of the tank side wall restricts the use of this geometry to applications in which the tank is completely full.

Experiments were conducted in this study to measure the mixing times in a bottom-pump-around liquid-jet-agitated tank for each of two jet arrangements. One arrangement involves a symmetric jet, and the other involves an asymmetric jet. The difference between the symmetric jet and the asymmetric jet is in the value of the side-angle. For the symmetric jet, the value of the side-angle is always 0°, whereas an asymmetric jet has some nonzero value for both the up-angle and the side-angle.

A schematic diagram of the experimental setup is shown in Figure 3. A flat-bottomed cylindrical tank, 296 mm in diameter and 296 mm in height, was used. The tank is made of Perspex glass. A pump-around, providing the liquid jet, takes suction from the tank base 25 mm from the tank wall and discharges a jet at an edge of the bottom face of the tank. This is referred to as the bottom-pump-around arrangement. A jet diameter of 18 mm and a 0.6-hp pump were used. For symmetric jet

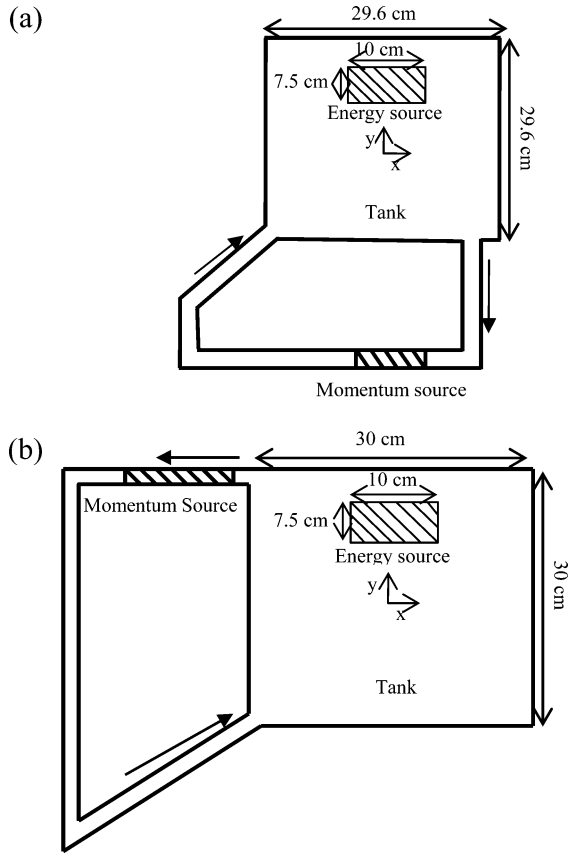

Figure 1. Two-dimensional view of (a) the tank geometry with a bottom-pump-around arrangement for the symmetric jet model of a liquid-jet-agitated tank and (b) the tank geometry with a side-pump-around arrangement used by Lane[1] and Ahmad.[19]

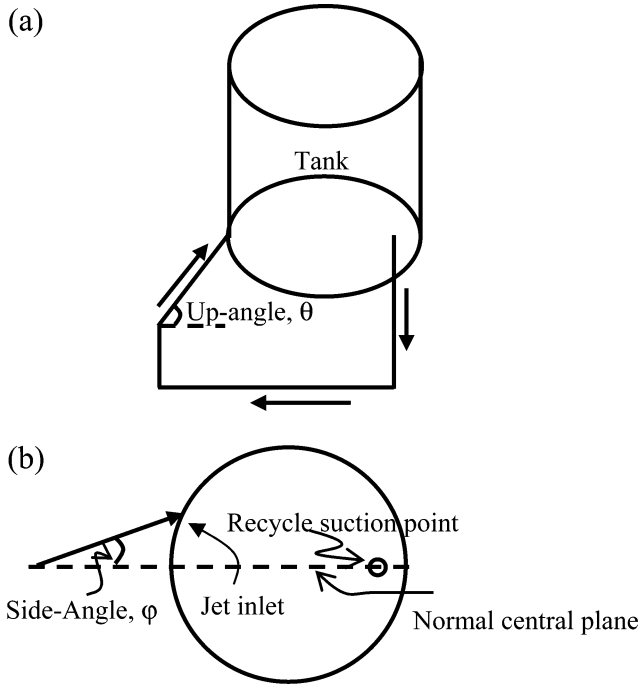

Figure 2. Schematic diagram of the angles that the jet makes with (a) the tank bottom, referred to as the up-angle, and (b) the central plane passing through the recycle suction point, referred to as the side-angle.

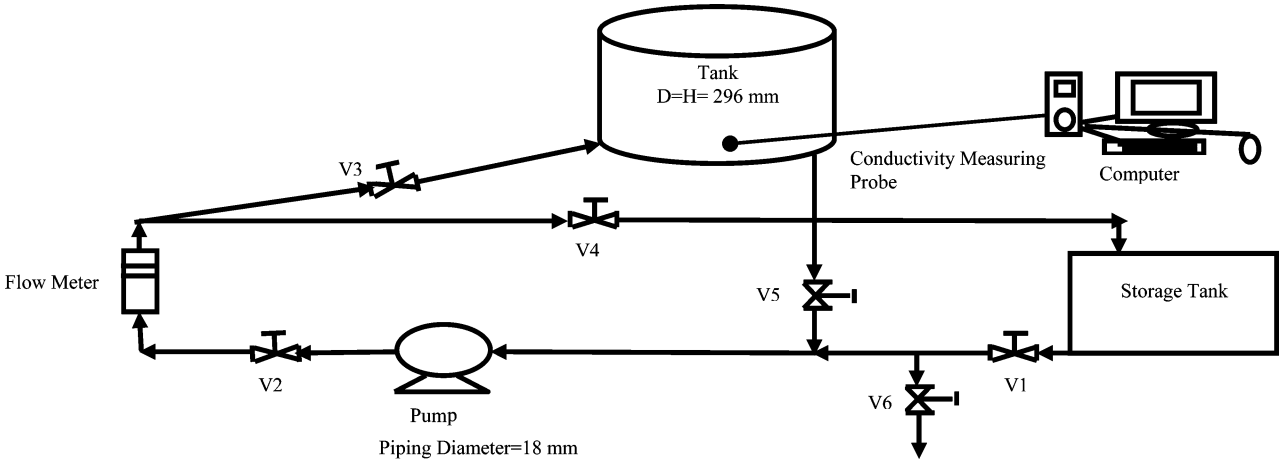

Figure 3. Schematic diagram of the experimental setup.

experiments, the jet had an up-angle of 45° and a side angle of 0°. The asymmetric jet experiments were carried out with an up-angle of 45° and a side-angle of 15°. A rotameter was used to measure the flow rate. This rotameter was calibrated prior to carrying out the experiments. The rotameter calibration was checked from time to time during this study to ensure the continuing accuracy of its readings. The tank was sealed and had a hole in its top cover for addition of the tracer.

A number of variables have been used by previous workers as the measured variables to quantify the degree of mixing. Lane and Rice,[9−11] Maruyama et al.,[12] Grenville and Tilton,[17] Perona et al.,[14] and Patwardhan[3] measured conductivity to quantify mixing. Conductivity was used in this experimental study as the measured variable. An Orion SensorLink conductivity system was used to measure conductivity. This system provides a convenient, reliable, and accurate method for measuring conductivity. It consists of an Orion SensorLink PCM 100 conductivity PCMCIA card, an Orion SensorLink cable to connect this card with an Orion conductivity cell model 11050 Epoxy 2-electrode, and an Orion SensorLink software to record the measurements in a computer. The PCM 100 card is inserted into a PCMCIA card dock of a computer. The conductivity of a solution with a specific electrolyte concentration changes with temperature. The probes provided with this system have an integral temperature sensor for a temperature range of 0−80 °C. Therefore, the measured values are automatically temperature-compensated. By definition, the temperature-compensated conductivity of a solution is the conductivity that the solution exhibits at the reference temperature. The reference temperature was chosen to be 25 °C for this study. The accuracy of the conductivity measurement is 0.5% of the full scale, whereas that of the temperature measurement is 1 °C.

A sodium chloride solution and dilute hydrochloric acid were tried as tracers. However, it was observed that hydrochloric acid has an operational advantage compared to sodium chloride, and it was used for most of the runs. The density of hydrochloric acid is less than that of a concentrated sodium chloride solution, and consequently, it interferes less when used as a tracer. A substantial increase in conductivity was achieved with the addition of only 5 mL of 7 M analytical reagent grade HCl. Sweet tap water was used as process water. Conductivity was measured using one probe at location A and one probe at location B as shown in Figure 4. These locations were determined using CFD simulations. These probe locations were expected to have the highest mixing times. Figure 4 also shows the location of points used to monitor mixing during the numerical runs. The position of the recycle suction point was also optimized using CFD[19] simulations, and a value of 25 mm was chosen. This selection will be explained further in a later section. For each value of the jet Reynolds number, the mixing time was measured three times. The averages of these values were used to validate the

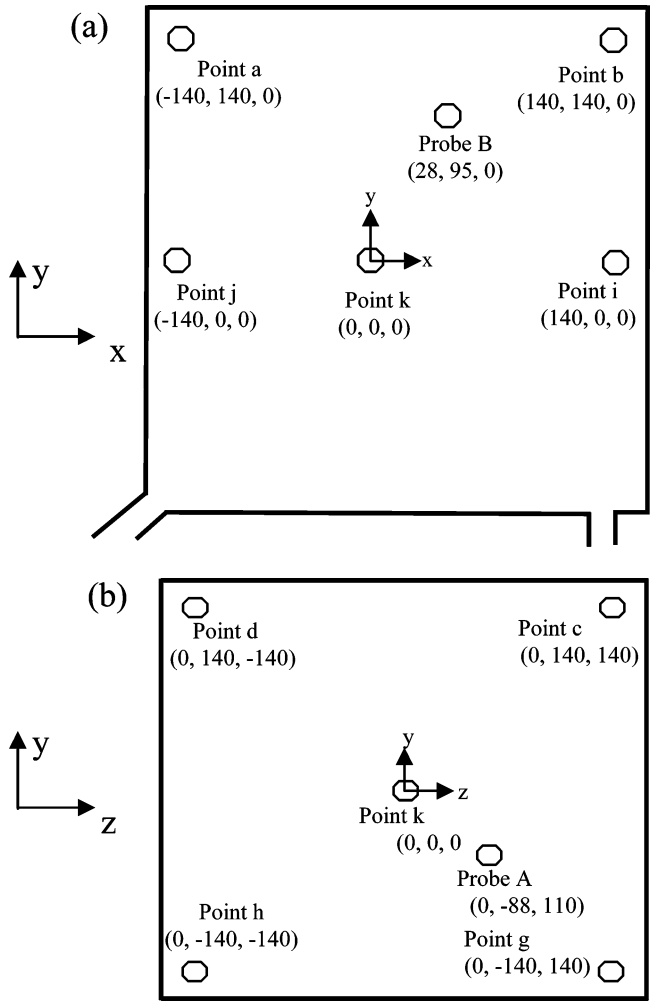

Figure 4. Location and coordinates, in mm, of 12 chosen monitoring points: (a) monitoring points in a central plane passing through the jet and (b) monitoring points in a central plane normal to the plane in a.

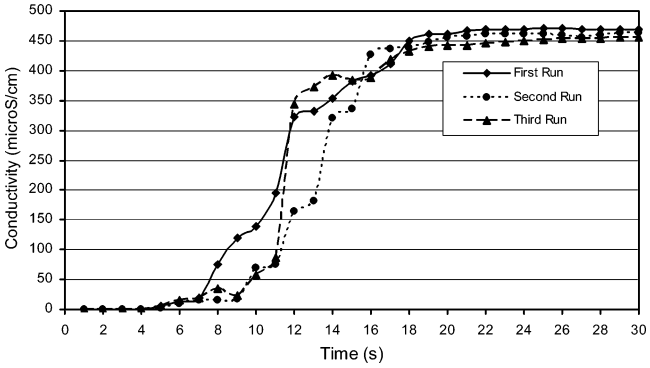

Figure 5. Plot of the conductivity versus time measured by probe A for a jet Reynolds number, N_{Rej}, of 32 166 for the symmetric jet tank.

numerical models. For validation purposes, the mixing time was calculated at exactly the same location as that of the experimental probe only and not at any other point. In the subsequent parametric numerical runs, mixing time was calculated based on achieving the desired degree of mixing in the whole tank, including all selected monitoring points. The locations of probes were selected on the basis of preliminary CFD simulations for one value of the jet Reynolds number. However, the time required to achieve 95% mixing in the whole tank is longer than that needed to achieve 95% mixing at the probe location. This difference might be more pronounced for jet Reynolds numbers other than the one that was used to define the probe location.

The results for these two bottom-pump-around tank jet arrangements, one involving a symmetric jet and the other an asymmetric jet, are discussed in the sections below. The results for the side-pump-around and bottom-pump-around tank geometries, both with a symmetric jet at an up-angle of 45°, are also compared in a later section.

Experimental Results for the Symmetric Jet Tank

Experimental runs were done for different jet Reynolds numbers, N_{Rej}. For each value of N_{Rej}, three experimental runs were carried out. Certain runs were repeated. Figure 5 shows the values of conductivity as a function of time, measured by probe A, for a jet Reynolds number of 32 166. These values are for three consecutive runs. Other runs showed a similar trend. There are some differences in the value of conductivity from one run to another. These differences are mainly due to slight changes in the initial conductivity and also experimental error. The times required to achieve 95% mixing in this case were 18, 20, and 18 s for the first, second, and third run, respectively. The average mixing time was 18.67 s. Thus, the maximum percentage error among these runs was 7% based on the average mixing time.

Figure 6 shows a plot of the experimental 95% mixing time, measured by probe A, as a function of N_{Rej}. The mixing time decreases as the jet Reynolds number is increased. The data also show a limited degree of scatter. Such scatter was also shown in the work of Lane and Rice,[10] who used a tank of about the same volume as the one used in this study. Perona et al.,[14] who used a tank much larger than the present one (about 20 times bigger) showed significantly more data scatter.

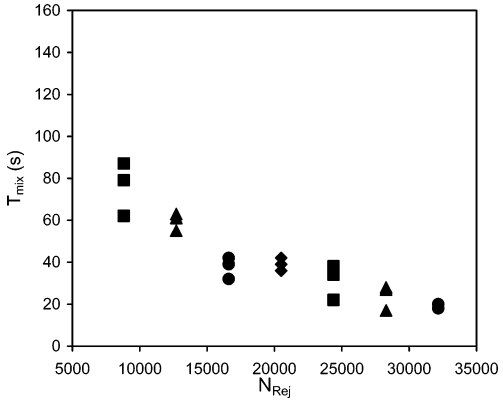

Figure 6. Plot of the mixing time determined experimentally by probe A as a function of N_{Rej} for the symmetric jet tank.

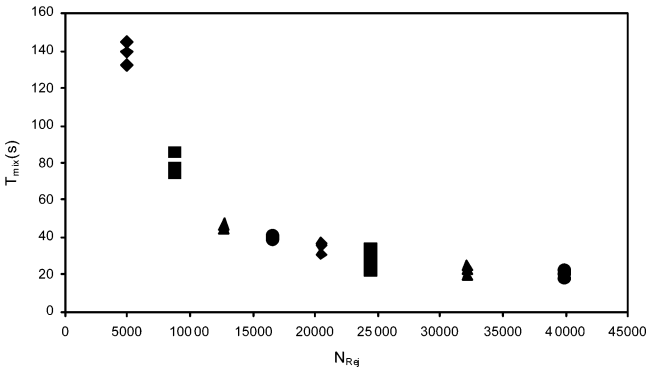

Figure 7. Plot of the mixing time determined experimentally by probe A as a function of N_{Rej} for the asymmetric jet tank.

Experimental Results for an Asymmetric Jet Tank

Another experimental setup was constructed as explained in the previous section. A tank and a pump-around of the same dimensions were used. The angle at which the jet was injected was the major difference between this setup and the previous one. In this case, the jet was not injected toward the tank center. The jet makes an angle with the vertical plane passing through the tank center and the pump-around off-take. This angle is referred to as the side-angle. The geometry used in this case had a side-angle of 15°. This angle was chosen with the aid of CFD simulations.[19] Preliminary CFD runs with a number of side-angles were performed, and an angle that was expected to yield the largest reduction in mixing time was chosen.

The locations of the two conductivity probes were carefully chosen again with the aid of CFD simulations. The positions were in the zones that were expected to experience the lowest velocity and consequently the slowest mixing. These positions were (0 mm, 290 mm, −140 mm) for probe A and (70 mm, 100 mm, 0 mm) for probe B, with the origin of the coordinates at the center of the tank bottom face. The raw data measured in this case are similar to those shown in Figure 5. For a jet Reynolds number of 28 278, the mixing times for three runs were 32, 30 and 31 s, respectively, giving an average mixing time for these runs of 31 s. The maximum percentage error was 3.2%, based on the average mixing time.

Figure 7 shows the plot of experimentally measured 95% mixing time as a function of the jet Reynolds number for the case with an asymmetric jet. The mixing time decreases as the jet Reynolds number increases.

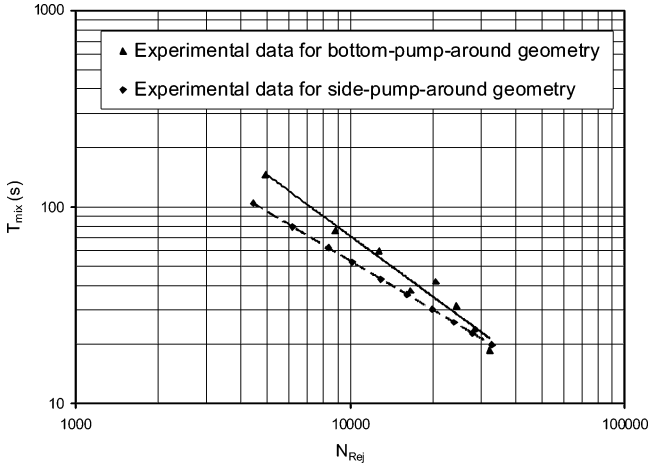

Figure 8. Plot of the experimental data for mixing time versus jet Reynolds number for bottom-pump-around and side-pump-around tank geometries, both having a symmetric jet.

It is also observed that the rate of decrease of the mixing time for the range $8000 < N_{Rej} < 16\,000$ is higher than that for the range $16\,000 < N_{Rej} < 28\,500$.

Comparison of Experimental Results

The experimental results obtained in this work for the bottom-pump-around tank geometry are compared with the experimental results by Lane and Rice[10] for the side-pump-around tank geometry. Both geometries involve a symmetric jet at an up-angle of 45°. Figure 8 shows this comparison. The time required to achieve 95% mixing for the side-pump-around geometry was found to be less than that for the bottom-pump-around geometry in the region of low jet Reynolds numbers. The times required for 95% mixing in the two geometries for Reynolds numbers greater than 25 000 were about the same. However, it should be kept in mind that Lane and Rice[10] measured conductivity at the monitoring point g or h shown in Figure 4b, whereas in this study, the monitoring point, probe A, was at a different location. This could lead to some differences in the measured mixing times. However, the side-pump-around geometry restricts the use of this setup to situations in which the tank is completely full, which is not always the case in industrial applications. As mentioned earlier, the bottom-pump-around tank geometry is more commonly used in industry.

The experimental results obtained in this work for the symmetric and asymmetric cases are rather limited by the fact that conductivity was measured at limited monitoring points, a maximum of two points. Although CFD was used to help determine the positions of the conductivity probes for one value of the jet Reynolds number, it is likely that this position might not be the one that gives the longest mixing time for all Reynolds numbers considered. For this reason, a comparison of the experimental data obtained for the symmetric and asymmetric jet models might not be conclusive. These experimental results are used to closely validate the numerical models by considering the values of the measured variable at exactly the same point experimentally and numerically. A thorough comparison of simulation results for the symmetric and asymmetric jet models is made in a later section.

Table 1. Mixing Times and Numbers of Cells for Different Mesh Interval Sizes for the Symmetric Jet Model

mesh size (mm)	no. of cells	mixing time (s)
12	88 587	32
11	100 813	30
10	116 186	26
9	134 608	26

Numerical Model of Mixing Using a Symmetric Jet

The bottom-pump-around tank geometry with the symmetric jet shown schematically in Figure 1a was simulated numerically. This is referred to as the symmetric jet model (SJM). Prior to obtaining the final 95% mixing times, the model was tested to establish that the model results were independent of grid size and time step size. Various turbulence models were also tested. A number of points were defined for monitoring mixing progress inside the tank. Detailed results were then obtained and compared with experimental results. These topics are discussed in detail in the following sections.

Effect of the Mesh Size. The only way to eliminate errors due to the coarseness of a grid is to perform a grid-dependence study. This is a procedure of successive refinement of an initially coarse grid until certain key results cease to change. To establish the grid independence of the numerical solution, geometries of the symmetric jet model for the liquid-jet-agitated tank were created with various mesh sizes, and the results were closely examined. When two mesh sizes produce a close result, the larger of the two should be chosen. The tank geometry created was discretized using mesh sizes of 12, 11, 10, and 9 mm. Table 1 lists the numbers of cells and the times required for 95% mixing to be achieved for the above-mentioned mesh intervals. The mesh used was tetrahedral and unstructured. This means that not all the cells are of the same volume and the number of cells cannot be directly deduced using the volume of the tank and the volume of the mesh cells because the volume of the cells is not constant.

Inspection of the velocity and temperature contour fields and comparison of them for different mesh interval sizes might not be an adequate approach for determining the grid independence of the solution. This is mainly due to the difficulty in observing minor differences in contour plots. Therefore, a line was defined at the tank center, i.e., at $z = 0$ mm, $y = 0$ mm, and $x = (-150)-150$ mm. The temperature values were recorded for equally spaced points along this line after 20 s for the tank geometries with mesh interval sizes given in Table 1. The flow field was fully developed at this time. From Figure 9, it can be seen that the curves for mesh interval sizes 10 and 9 mm nearly coincide. The maximum difference between these curves is only 0.02% based on a mesh interval size of 10 mm. Furthermore, the mixing times for the mesh interval sizes of 10 and 9 mm are the same, i.e., 26 s. Thus, it was decided to choose a mesh interval size of 10 mm for the symmetric jet model in order to economize on the computational time needed to obtain converged results.

Effect of the Time Step Size. The geometry for the symmetric jet model of a liquid-jet-agitated tank with a mesh interval size of 10 mm was run for time steps of 2, 1, and 0.5 s. A line was defined at the tank center, i.e., at $z = 0$ mm, $y = 0$ mm, and $x = (-150)-150$ mm.

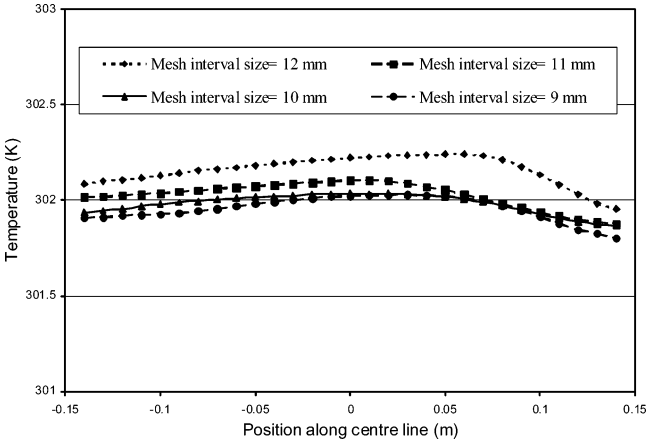

Figure 9. Plot of the temperature along the center line for the symmetric jet model tank geometry meshed using different mesh interval sizes.

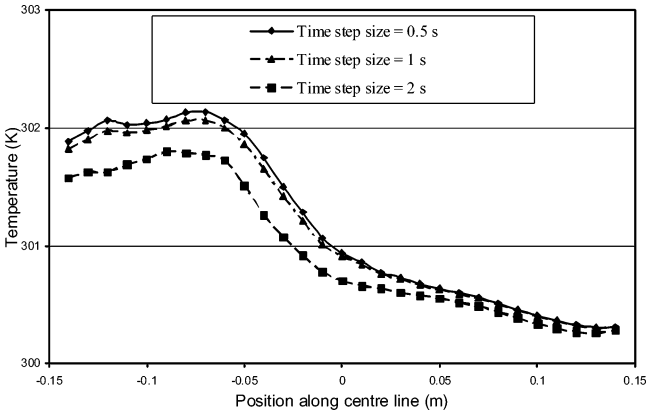

Figure 10. Effect of the size of the time step on the numerical solution of the symmetric jet model for the liquid-jet-agitated tank geometry with mesh interval size of 10 mm.

Temperature values were recorded along this line after 6 s for each of the above-given time steps, and the results are shown in Figure 10. A time of 6 s was chosen because the flow does not become developed until this time. The curves for the time step sizes of 0.5 and 1 s nearly coincide. The maximum difference between two points on these curves for the same on-line position is 0.03% based on a time step of 1 s. The mixing times for the time steps of 1 and 0.5 s are the same, i.e., 26 s, whereas that for a time step of 2 s is 32 s. Consequently, it was decided to use a time step of 1 s.

Effect of the Tank Outlet Position. It was observed that, if the recycle suction is located 50 mm from the tank wall, then the low velocity zones near the tank bottom are larger than in the case when the suction is located 25 mm from the tank wall. Because of these low-velocity zones, the mixing time is longer for the tank geometry with the outlet at 50 mm from the tank wall, as shown in Figure 11. Therefore, a tank outlet at a distance of 25 mm from tank wall was used in this study.

Other outlet positions were tested, but because of the small difference in mixing time shown in Figure 11 and the disappearance of the low-velocity zone between the outlet and the near wall of the tank for an outlet location at 25 mm, the choice of 25 mm is justified, and bringing the outlet position closer to the wall did not have any further significant effect on the mixing time.

Effect of the Turbulence Model. Simulations of mixing in a tank agitated with a symmetric jet were

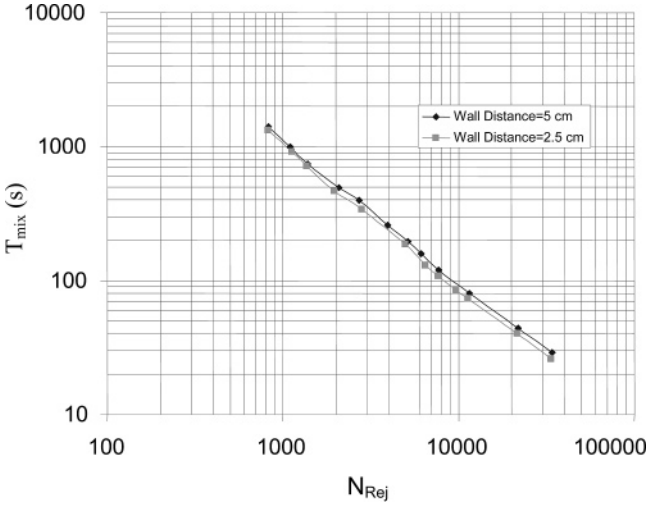

Figure 11. Plot of 95% mixing time, T_{mix}, versus jet Reynolds number, N_{Rej}, for the recycle suction point located at distances of 50 and 25 mm from tank wall.

carried out using a number of different turbulence models. The standard $k-\epsilon$ model, the realizable $k-\epsilon$ model, the renormalization group (RNG) $k-\epsilon$ model, and the Reynolds stress model (RSM) were used to investigate the effects of these models on the simulation results. The same geometry was used for all these cases. A momentum source of the same value was used for every model. The results for the standard $k-\epsilon$ model and the realizable $k-\epsilon$ model were similar. The 95% mixing time was 26 s for both models, and the monitoring point g was the last mixed. For the RNG $k-\epsilon$ model, the mixing time was 23 s, with monitoring points h and probe A mixed last. The RSM model gave the highest mixing time of 28 s, with point h as the last point where 95% mixing was achieved.

The $k-\epsilon$ model has been used to simulate jet mixing in tanks by many previous researchers, including Zughbi and Rakib,[8,16] Patwardhan,[3] and Jayanti.[15] It was also successfully used to simulate mixing in a pipeline with a side-tee by Zughbi et al.[20] This model was found to give reasonable results away from the vicinity of the jet. The RSM is the most sophisticated of the four turbulence models tested. However, because of a significant increase in the CPU time and limited improvement in results, the standard $k-\epsilon$ model was used for most of the results presented in the following sections.

Validation of the CFD Symmetric Jet Model. Figure 12 shows a plot of the average mixing times measured experimentally by probe A for jet Reynolds numbers ranging from 5000 to 32 000. Mixing times obtained numerically by monitoring the tracer values at a point identical to the location of probe A for different jet Reynolds numbers are also plotted in this figure. Experimental and numerical results show excellent agreement, and the difference between the two is less than 7%. The numerical model can now be considered to be validated and can be used to carry out different parametric runs. It should be noted that the numerical results were obtained for 95% mixing at a single location identical to the location of the experimental probe and not for the whole tank. The values of the mixing time reported in Figures 18 and 24 below indicate when 95% mixing was achieved in the whole tank, including all monitoring points shown in Figures 4 and 13. Although efforts were made to place probe A in a slow-mixing

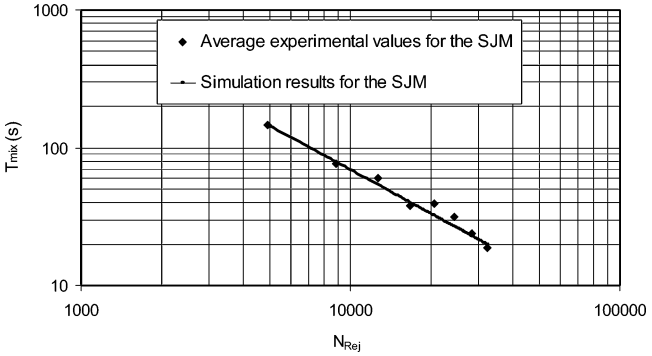

Figure 12. Plot of mixing time measured experimentally and determined numerically at the same location, probe A, for different values of jet Reynolds number for the symmetric jet model.

location, this turned out to be not the location with the slowest mixing (longest mixing time).

Numerical Asymmetric Jet Model

For the asymmetric jet model (AJM), a geometry representing a bottom-pump-around tank with an asymmetric jet, i.e., an up-angle of 45° and a side-angle of 15°, was constructed. A number of points were selected to monitor the progress of mixing. These monitoring points were chosen to represent zones with the lowest velocities, i.e., with the longest mixing times. They were selected with the help of CFD simulations. Figure 13 shows the locations of the points defined to monitor the degree of mixing for the asymmetric jet model. It should be noted that the origin of the system of coordinates in this case was chosen to be at the center of the tank base. For the symmetric case, the origin was at the center of the tank. There is no physical significance for this difference, and it does not have any impact on the solution.

To establish the grid independence of the numerical solution for the asymmetric jet model, the tank geometry created was discretized using mesh interval sizes of 10, 9, 8, and 7 mm. Table 2 lists the numbers of cells for the above-mentioned mesh intervals. Because an unstructured mesh is used, the volumes of the cells could vary, and consequently, the total numbers of cells for similar volumes could vary depending on the details of the volume. This explains the difference in the total numbers of cells in Tables 1 and 2 for the same mesh size. A line was defined at the tank center, i.e., at z = 0 mm, y = 150 mm, and x = (−150)−150 mm. The temperature values were recorded for all equally spaced points on this center line, 10 s after the flow was started, for the tank with the mesh interval sizes given in Table 2. The flow field was developed at this time. Figure 14 shows temperature plots along this center line for the four cases of different mesh sizes.

Figure 14 shows that the curves of the mesh interval sizes of 8 and 7 mm nearly coincide. The maximum difference between these curves at the most distant points is only 0.04% based on a mesh interval size of 8 mm. Furthermore, the mixing times for the mesh interval sizes of 8 and 7 mm were the same, i.e., 17 s. Consequently, a mesh interval size of 8 mm was chosen for this case, the asymmetric jet model, to economize on the computational time.

The tank geometry with a mesh interval size of 8 mm for the asymmetric jet model of a liquid-jet-agitated tank was run for time step sizes of 2, 1, and 0.5 s. A line was

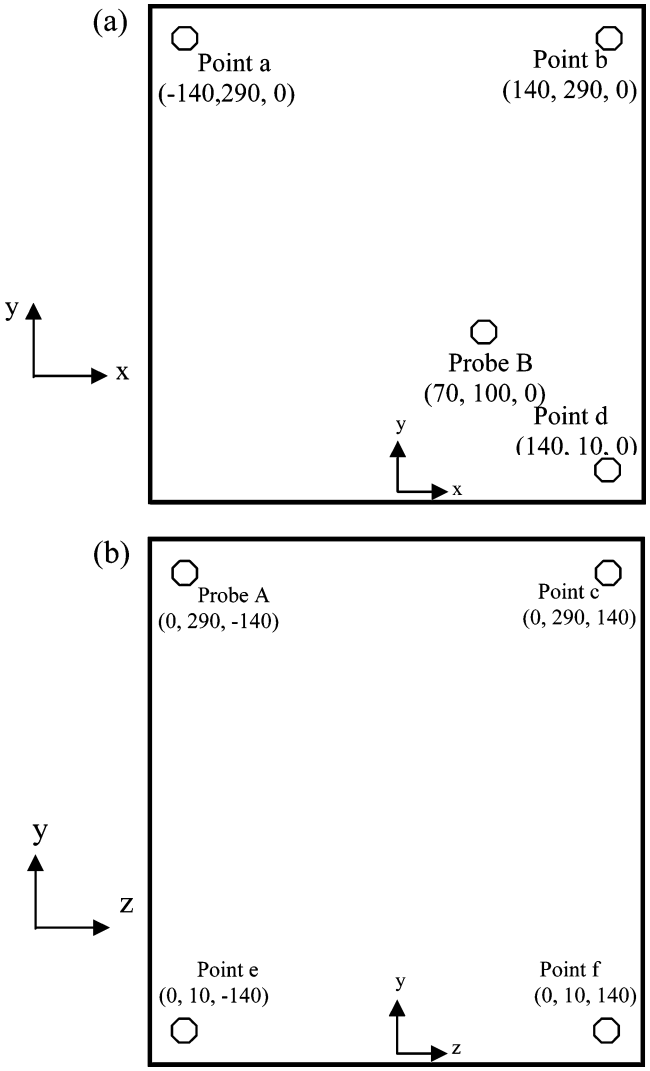

Figure 13. Locations of the monitoring points for the asymmetric jet model of liquid-jet-agitated tank (the coordinates are in mm).

Table 2. Mixing Time and Number of Cells for Different Mesh Interval Sizes for an Asymmetric Jet Model

mesh size (mm)	no. of cells	mixing time (s)
10	126 207	20
9	184 759	22
8	252 801	17
7	345 330	17

defined at the tank center, i.e., at z = 0 mm, y = 150 mm, and x = (−150)−150 mm. The temperature was recorded along this center line after 6 s for each of the above time step sizes. A plot of temperature versus distance along the central line in a horizontal plane is shown in Figure 15. A time of 6 s was chosen because the flow does not become fully developed until this time. The curves for the time step sizes of 0.5 and 1 s nearly coincide. The maximum difference between any two points on these curves for the same position on the line is 0.07% based on a time step size of 1 s. The mixing times for the time step sizes of 1 and 0.5 s are the same, i.e., 17 s, whereas that for a time step size of 2 s is 21 s. It was therefore decided to use a time step size of 1 s.

Validation of the CFD Asymmetric Jet Model. Figure 16 shows a plot of the mixing time at the location probe A measured both experimentally and numerically for different jet Reynolds numbers. The two sets of results are in good agreement. The error bars shown

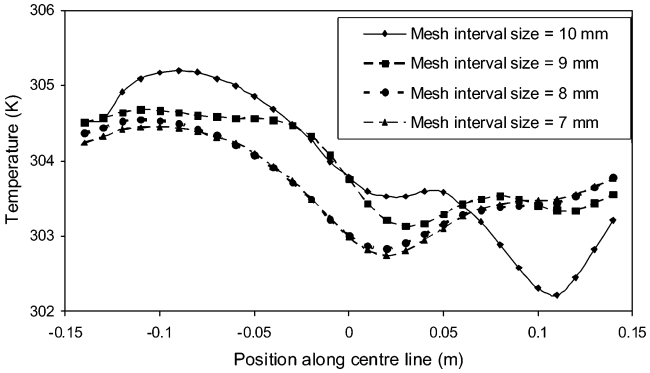

Figure 14. Plot of temperature along the center line for the asymmetric jet model tank geometry meshed using different mesh interval sizes.

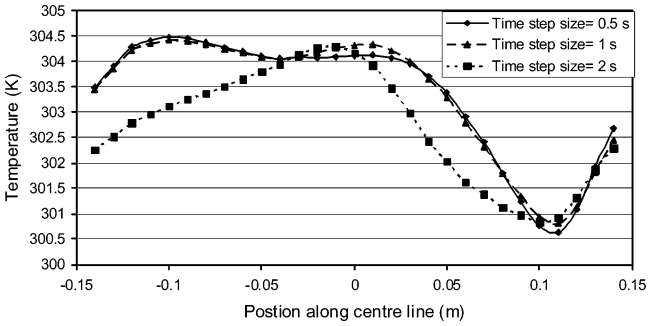

Figure 15. Effect of the size of the time step on the numerical solution of the asymmetric jet model for the liquid-agitated tank with a mesh interval size of 8 mm.

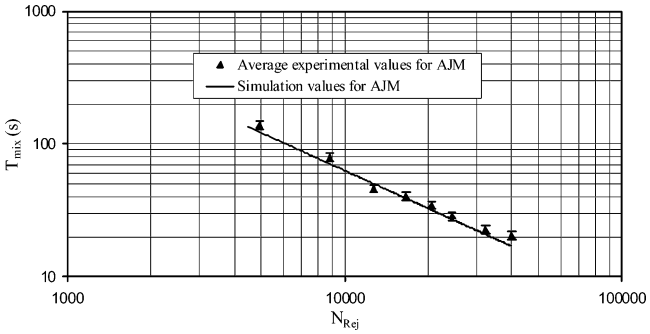

Figure 16. Plot of mixing time measured experimentally and determined numerically at the same location, probe A, for different values of jet Reynolds number for the asymmetric jet model.

correspond to 7% error. This validates the asymmetric jet model and the model can now be used to carry out different parametric runs.

Comparison of Side-Pump-Around and Bottom-Pump-Around Geometries

The objective of this study is to ultimately provide information that will contribute toward an optimum design of liquid-jet-agitated tank mixers. Therefore, the simulation results of the geometry used by Lane and Rice,[11] referred to as the side-pump-around geometry, are compared with those of the bottom-pump-around geometry, both having a symmetric jet with an up-angle of 45°. Figure 17 shows a comparison of the simulation results by Zughbi and Rakib[8] for a side-pump-around geometry with the simulation results obtained during this study for a bottom-pump-around geometry.

The location of probe A for the symmetric jet model is shown in Figure 4, and the probe location for the asymmetric model is shown in Figure 13. These locations were selected on the basis of some limited CFD runs at one specific Reynolds number. The probes are not at identical locations, and because the simulation results show that the SJM and AJM flow patterns are entirely different, a comparison of these experimental results will not be meaningful. The purpose of the experiments was to validate the numerical models that were subsequently used for further detailed studies.

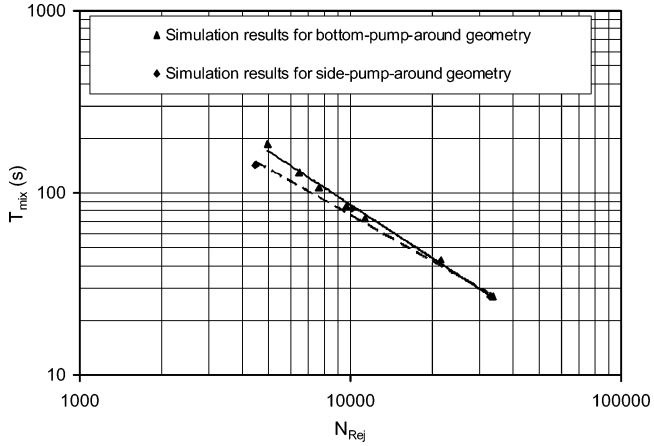

Figure 17. Mixing time obtained from simulation for different jet Reynolds numbers for the Lane and Rice geometry[11] and the symmetric jet model geometry.

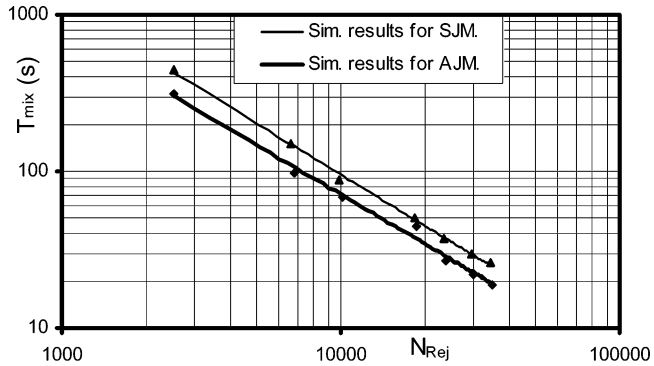

Figure 18. Comparison of mixing times for the symmetric jet model and asymmetric jet model geometries.

Figure 17 shows that the simulation results of both side- and bottom-pump-around do not differ significantly over a jet Reynolds number range of 10 000−32 000. A trend similar to that observed in Figure 8 is also observed for $N_{Rej} < 25\,000$. The time required to achieve 95% mixing for the side-pump-around geometry is found to be slightly shorter than that for the bottom-pump-around. For $N_{Rej} > 25\,000$, the simulated 95% mixing times for the two geometries are almost the same. The side-pump-around geometry restricts the use of this setup to cases when the tank is completely full, which is not always the case in industrial applications.

Comparison of Simulation Results for Symmetric and Asymmetric Jet Models

Figure 18 shows a comparison of 95% mixing times for symmetric and asymmetric tank geometries with the bottom-pump-around setup for different jet Reynolds numbers. The diameter of the tank used in this simulation study is 296 mm, with piping of diameter 18 mm for both model geometries. The up-angle for both geometries is 45°. The side-angle for the asymmetric jet

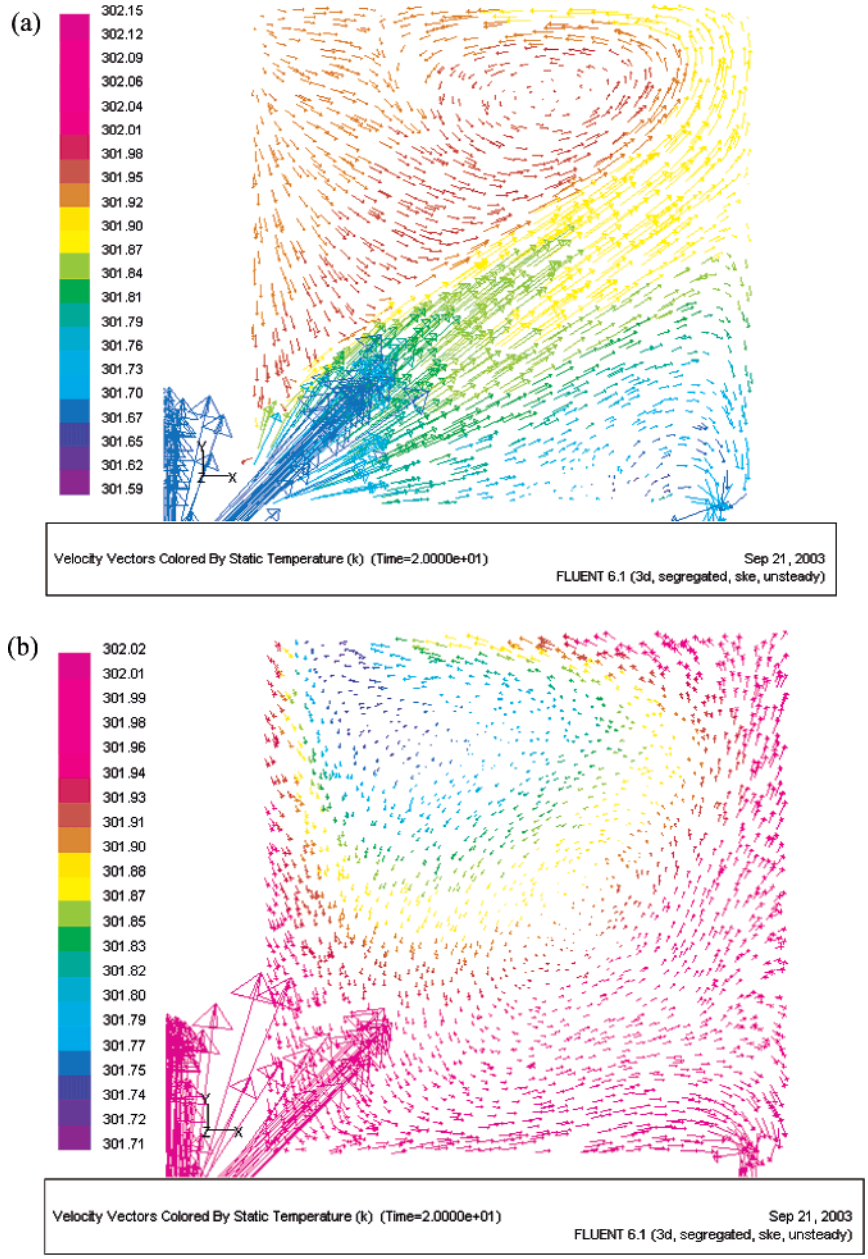

Figure 19. Velocity vectors colored by the magnitude of temperature in a central plane passing through the recycle suction point for a bottom-pump-around tank geometry with (a) a symmetric jet and (b) an asymmetric jet.

is 15°. A reduction of between 12% and 34% in mixing time is achieved by using the asymmetric jet. This result implies that, when an asymmetric jet is used, the flow patterns inside the tank tend to differ significantly from the case with a symmetric jet. Consequently, the 95% mixing time is different. Figures 19 and 20 show a comparison of the flow patterns in two vertical central planes for the symmetric and asymmetric jet tanks. The value of the jet Reynolds number is 39 000. These figures show the velocity vectors colored by the temperature values in the respective planes at a time of 20 s. These figures show the significant effect of flow patterns on mixing time. They are in line with the findings of Zughbi and Rakib[8] and Maruyama.[7] These findings contradict those of Okita and Oyama,[21] who stated that the mixing time is independent of the angle of the jet and, consequently, independent of the flow patterns.

Effect of the Jet Up-Angle on Mixing Time for a SJM

In the context of the above-cited work, simulations were carried out to investigate the effect of different jet up-angles on mixing time for a symmetric jet model (SJM) of a liquid-jet-agitated tank. The tank geometry shown in Figure 1a was used. First, the values of the measured variable, the temperature, were recorded for the monitoring points shown in Figure 4. However, it was observed that a small change in the jet up-angle affected the flow field and, hence, the temperature values at the monitoring points. As an example, the mixing times based on these monitoring points were 42 and 56 s for jet up-angles of 58° and 60°, respectively. The velocity vectors for the low-velocity range, in the $y-z$ plane, are shown in Figure 21 for the above-given angles. The last-mixed point for the 60° angle geometry is g, which lies in the $y-z$ plane at the right bottom

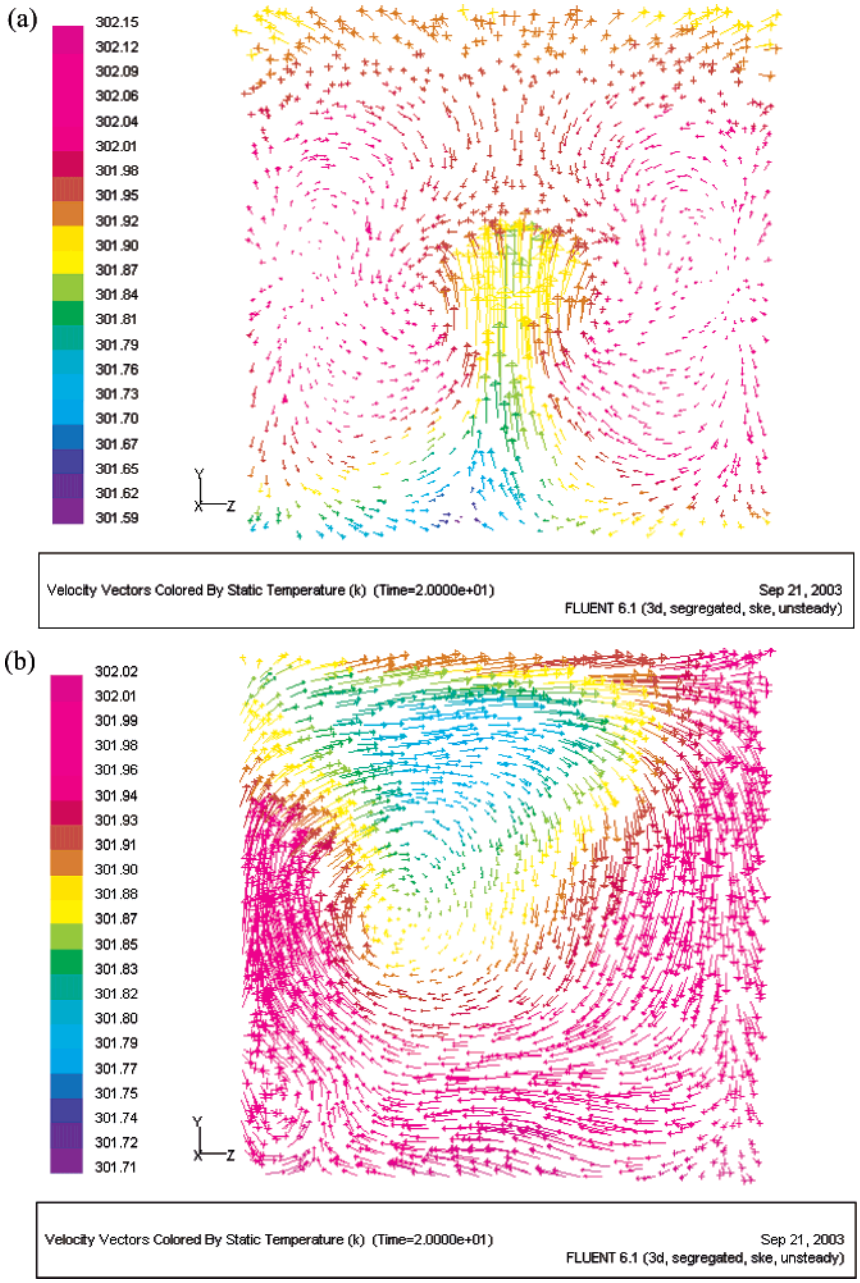

Figure 20. Velocity vectors colored by the magnitude of temperature in a plane normal to that in Figure 19 for a bottom-pump-around tank geometry with (a) a symmetric jet and (b) an asymmetric jet.

corner. It can be seen that the value of the velocity at this point g for the up-angle of 60° is less than that for the up-angle of 58°. This is the reason significantly different mixing times were obtained for a small change in the jet up-angle. Therefore, it was decided to use the minimum and maximum values of the measured variable, the temperature, in the bulk tank liquid for mixing time calculations. Figure 22 shows the mixing time for 95% mixing for different jet up-angles. For the bottom-pump-around geometry used in this study, a jet up-angle of 20° gives the lowest mixing time. The 95% mixing time is a strong function of the flow patterns. These patterns are, in turn, a strong function of the jet up-angle. As a result, many local maxima and minima are shown in Figure 22.

The dependence of the 95% mixing time on the jet up-angle in a bottom-pump-around is somewhat similar to that of a side-pump-around discussed by Zughbi and Rakib.[8] The similarity arises from a similar explanation for the two phenomena. This explanation states that, at 45°, the jet might dissipate before it impinges on the opposite corner and, if it does, it splits into two weak subjets because of its symmetry. When the angle is made smaller or larger than 45°, the jet impinges on the opposite side or top wall and connects with this boundary, creating a stronger circulating flow in the tank. This explanation does not challenge the basic concept of mixing. The concept states that the mixing is achieved by a liquid jet, and as this jet penetrates the primary or slow-moving liquid, the jet entrains at its boundaries some of that primary liquid. What this explanation challenges is the concept that a jet injected along the diagonal of a tank with an aspect ratio of 1 produces the greatest jet length and consequently the shortest mixing time.

The Coldrey design[6] depends on a limited definition of the jet length. A jet that hits a side wall and continues to flow is more effective for mixing than a jet that flows

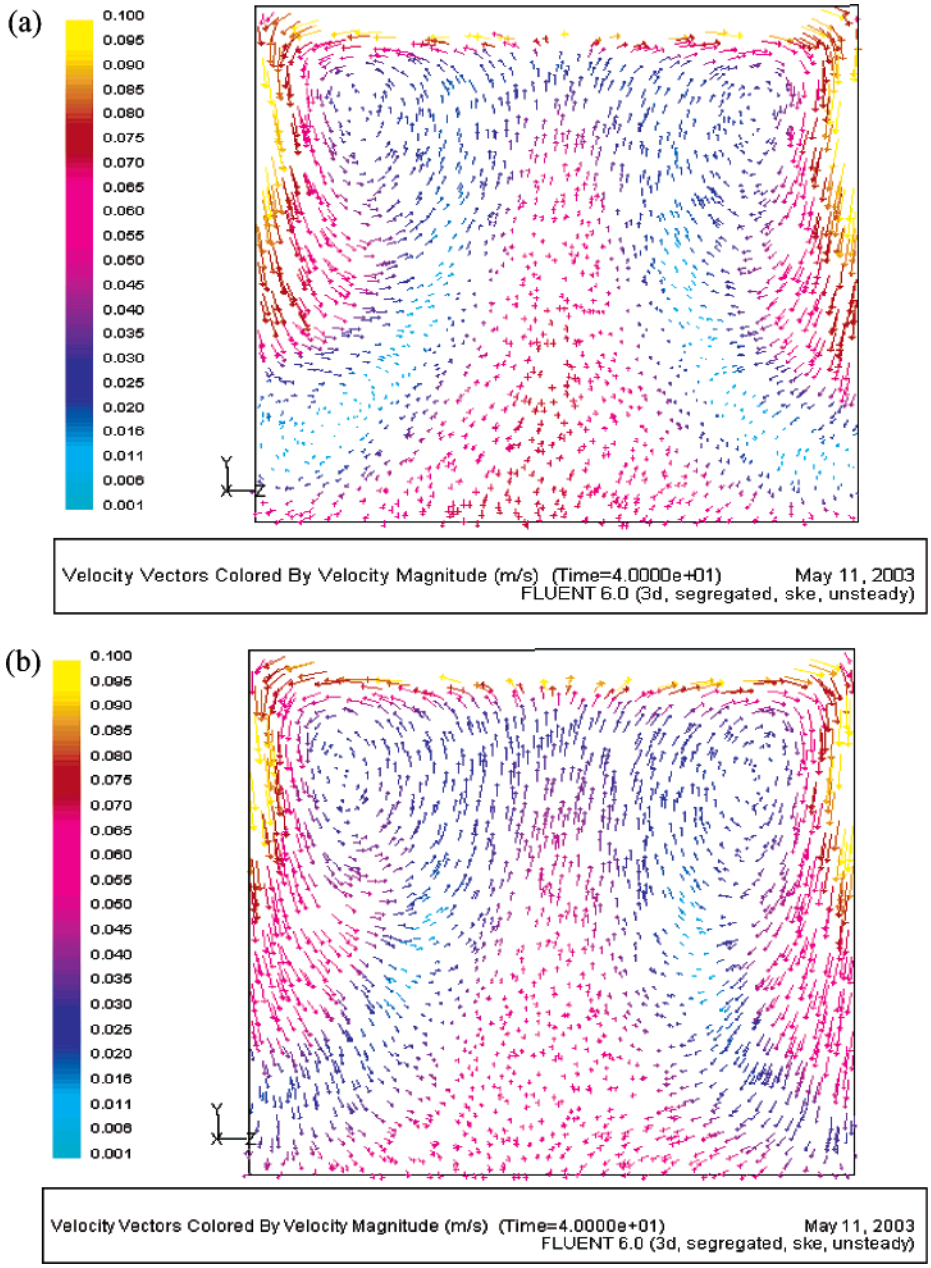

Figure 21. Velocity vectors for the symmetric jet model of a liquid-jet-agitated tank with a bottom-pump-around geometry and a jet up-angle of (a) 60° and (b) 58°.

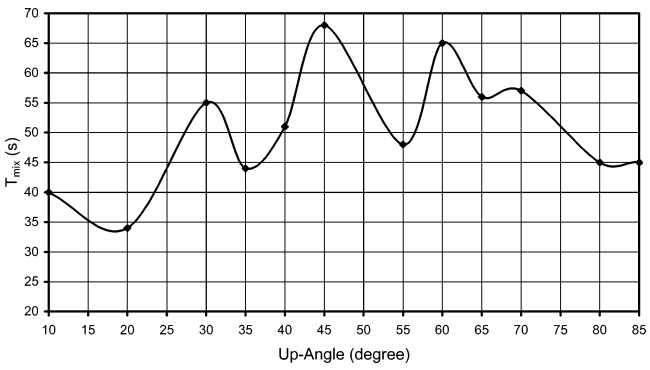

Figure 22. Effect of different values of jet up-angle on mixing time for the symmetric jet model of a liquid-jet-agitated tank.

along a tank diagonal and fails to connect, as effectively, with a side wall.

The flow patterns created inside the tank vary with varying jet arrangements. Consequently, the size and extent of the low-velocity zones and the mixing time vary with varying flow patterns.

Effect of Jet Side-Angle on Mixing Time for an AJM

In the comparison of the 95% mixing times for the symmetric jet model (SJM) and asymmetric jet model (AJM), it was mentioned that the AJM gave a reduction of up to 34% in mixing time. The jet up-angles for the two model geometries are the same, i.e., 45°, whereas the jet side-angle for the AJM is 15°. Figure 23 shows a plot of the mixing time as a function of side-angle. The diameter of the tank was 296 mm, and that of the piping was 20 mm. A jet side-angle of 15° appears to give the minimum time.

It should be noted that this side-angle is not universal, i.e., for a tank of different dimensions, the optimum side-angle might be different from 15°. However, the

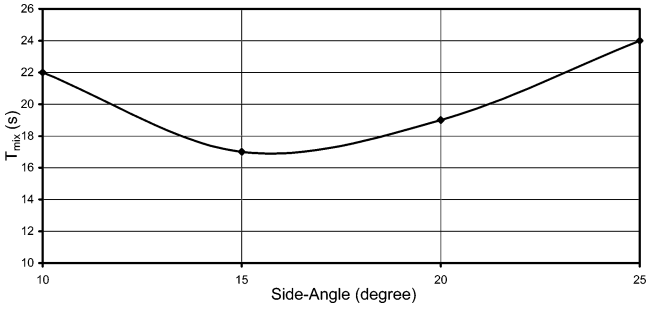

Figure 23. Plot of 95% mixing time for different jet side-angles for the asymmetric jet model of a liquid-jet-agitated tank with a bottom-pump-around geometry.

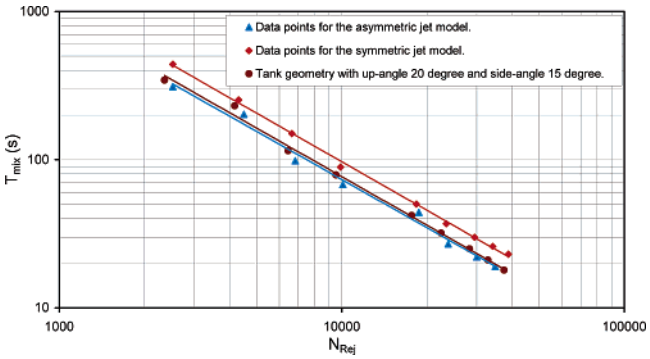

Figure 24. Plot of 95% mixing time for the symmetric jet model geometry, the asymmetric jet model geometry, and a geometry with an up-angle of 20° and a side-angle of 15° for different jet Reynolds numbers.

contribution of asymmetry to better mixing should be true for all cases.

Combined Effect of Side-Angle and Up-Angle: An Optimum Design

It was mentioned in previous sections that a jet up-angle of 20° for the symmetric jet model and a jet side-angle of 15° for the asymmetric jet model gave the lowest mixing times. Therefore, it was decided to test the effect of combining these two angles. Hence, a bottom-pump-around tank geometry with a jet up-angle of 20° and a jet side-angle of 15° was generated. The diameter of the tank was 296 mm, and that of the piping was 18 mm. Figure 24 shows a plot of the 95% mixing time versus the jet Reynolds number for the symmetric jet model with a jet up-angle of 45°, the asymmetric jet model with a jet having an up-angle of 45° and a side-angle of 15°, and a geometry with the jet coming in at an up-angle of 20° and a side-angle of 15°. This figure clearly shows that the reduction in mixing time due to the side- and up-angles is not additive. The geometry with the jet injected at the optimum side- and up-angles did not produce a mixing time shorter than that produced by the geometry with the optimum side-angle only.

Effect of Aspect Ratio on 95% Mixing Time

The work that has been reported so far in this study is for a tank with an aspect ratio of 1.0. Grenville and Tilton[17] suggested that an aspect ratio of $1/\sqrt{2}$ would give a shorter mixing time. This effect of aspect ratio on mixing time is investigated using CFD in this section. A tank with an aspect ratio of $1/\sqrt{2}$ having the same volume as a tank with a diameter of 296 mm and a

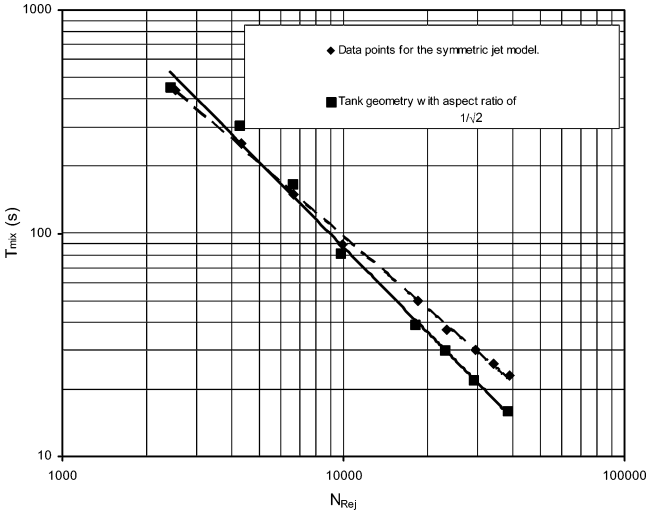

Figure 25. Plot of 95% mixing time for the SJM geometry and for the geometry with an aspect ratio of $1/\sqrt{2}$ for different jet Reynolds numbers.

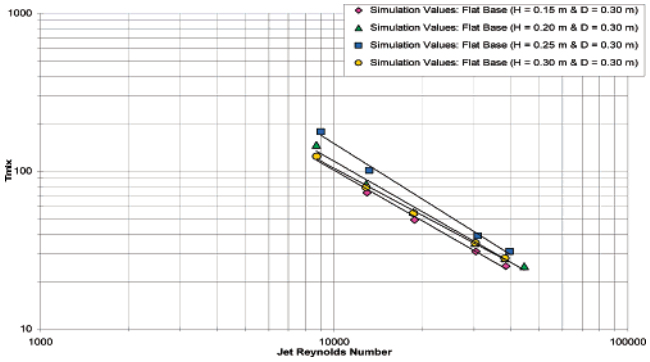

Figure 26. Plot of the 95% mixing time for various liquid heights in the tank.

height of 296 mm was constructed. The diameter of this tank is 332.3 mm, and its height is equal to 235 mm. The diameter of the pump-around pipe for this tank was the same as used for SJM and AJM geometries, i.e., 18 mm. The value of the jet up-angle for this geometry is 45°, whereas the jet side-angle is 0°. Figure 25 shows that the tank with an aspect ratio of $1/\sqrt{2}$ gave a mixing time shorter than that of the symmetric jet geometry for $N_{Rej} > 7000$. The symmetric jet geometry has an aspect ratio of 1.

Simulations were also carried out for a tank with a diameter of 296 mm and liquid heights of 150, 200, and 250 mm, respectively. Figure 26 shows a plot of the 95% mixing time obtained from simulation versus jet Reynolds number for various *H*/*D* ratios. It should be noted that the volume of liquid was different in each of these cases. It is observed that the 95% mixing times for the liquid heights of 200 and 250 mm are higher than that of the 300-mm case. The mixing time for the 150-mm liquid height is slightly lower than that for 300 mm. It can be concluded that the mixing time is a strong function of the aspect ratio and a weaker function of the volume of the tank.

Conclusions

Numerical and experimental investigations of mixing in liquid-jet-agitated tanks were carried out. These tanks have a bottom-pump-around arrangement for introducing the liquid jet. A comparison was made with

a tank having a side-pump-around arrangement. The liquid jet mixing in this tank was investigated experimentally by Lane and Rice[10] and numerically by Zughbi and Rakib.[8,16] On the basis of the current investigations, the following conclusions can be made:

The location of the pump-around suction point was found to have some effect on the mixing time, and it was optimized using CFD results. The optimum location was found to be at 25 mm from the wall of the tank. Experimental and numerical values of the 95% mixing time for mixing in a liquid-jet-agitated tank showed good agreement. This agreement was observed for a bottom-pump-around geometry with a symmetric jet and for a bottom-pump-around arrangement with an asymmetric jet.

Experimental and numerical results showed that the 95% mixing time for a side-pump-around geometry is slightly lower than that for a bottom-pump-around arrangement for N_{Rej} values less than 25 000. For higher values of N_{Rej}, the mixing times were almost the same. However, the bottom-pump-around arrangement remains favored for industrial use because it can be used when the tank is only partly full.

The flow asymmetry was found to have a significant effect on the 95% mixing time, because the mixing time is dependent on the flow patterns inside the tank. Simulation results showed that the 95% mixing time in a tank having a bottom-pump-around arrangement with an asymmetric jet was found to be about 17% lower than the mixing time in a similar tank with a symmetric jet.

For the bottom-pump-around geometry with a symmetric jet, a jet up-angle of 20° resulted in the lowest mixing time based on the 95% mixing criteria. This mixing time was 50% shorter than that of a symmetric jet with an up-angle of 45°.

For the bottom-pump-around geometry with an up-angle of 45°, a side-angle of 15° resulted in the lowest mixing time. This mixing time was 29% less than that obtained for an up-angle of 45° and a side-angle of 25°.

A geometry in which the jet had both optimum up- and side-angles did not result in any further improvement on what was achieved with either the optimum side- or up-angle.

The aspect ratio of the tank was also found to have an impact on the mixing time. An aspect ratio of $1/\sqrt{2}$ was found to give a shorter 95% mixing time than the symmetric jet geometry for Reynolds numbers larger than 7000.

Acknowledgment

The authors acknowledge the financial support of KFUPM, Project CHE/MIX/253, for this work.

Nomenclature

C = concentration of tracer anywhere in the tank, g/L
$\bar{C}$ = final mean tracer concentration, g/L
d = diameter of the jet, mm
D = diameter of the tank, mm
H = height of the liquid in the tank, mm
m = constant used as a mixing criterion, $m=|(C - \bar{C})/\bar{C}| < 0.05$
P = pressure in the equations of motion (including gravitational acceleration where applicable), Pa
Re = Reynolds number
t_{95} = time required to reach 95% mixing, s
T = Temperature anywhere in the tank, K
$\bar{T}$ = Final mean temperature, K
v_x = velocity in the x direction, m/s
v_y = velocity in the y direction, m/s
v_z = velocity in the z direction, m/s

Greek Letters

φ = side-angle, angle the jet makes with a vertical plane passing through the jet outlet and the axis of the tank, deg
θ = up-angle, angle the jet makes with a horizontal plane parallel to the tank base, deg
ρ = density of the fluid, kg/m^3
μ = viscosity of the fluid, Pa.s

Literature Cited

(1) Lane, A. G. C. Liquid Jet Mixing in Tanks. Ph.D. Dissertation, Department of Chemical Engineering, Loughborough University of Technology, Leicestershire, U.K., 1981.

(2) Harnby, N., Edwards, M. F., Nienow, A. W., Eds. *Mixing in the Process Industries*; Butterworth-Heinemann: London, 1985.

(3) Patwardhan, A. W. CFD Modeling of Jet Mixed Tanks. *Chem. Eng. Sci.* **2002**, *57*, 1307.

(4) Fossett, H.; Prosser, L. E. The Application of Free Jets to the Mixing of Fluids in Bulk. In *Proc. Inst. Mech. Eng.* **1949**, *160*, 224−251.

(5) Fox, E. A.; Gex, V. E. Single-Phase Blending of Liquids. *AIChE J.* **1956**, *2*, 539.

(6) Coldrey, P. W. Paper to IChemE Course, University of Bradford, Bradford, U.K., 1978.

(7) Maruyama, T. Jet Mixing of Fluids in Vessels. In *Encyclopedia of Fluid Mechanics*; Gulf Publishing Company, Houston, TX, 1986; Vol. 2, pp 544−556.

(8) Zughbi, H. D.; Rakib, M. A. Investigations of Mixing in a Fluid Jet Agitated Tank: Effects of Jet Angle and elevation and Number of Jets. *Chem. Eng. Sci.* **2004**, *59*, 829.

(9) Lane, A. G. C.; Rice, P. An Experimental Investigation of Liquid Jet Mixing Employing a Vertical Submerged Jet. *Proc. Inst. Chem. Eng. Symp. Ser.* **1981**, *64*, K1−K14.

(10) Lane, A. G. C.; Rice, P. The Flow Characteristics of a Submerged Bounded Jet in a Closed System. *Trans. Inst. Chem. Eng.* **1982**, *60*, 245.

(11) Lane, A. G. C.; Rice, P. An Investigation of Liquid Jet Mixing employing an Inclined Side Entry Jet. *Trans. Inst. Chem. Eng.* **1982**, *60*, 171.

(12) Maruyama, T.; Ban, Y.; Mizushina, T. Jet Mixing of Fluids in Tanks. *J. Chem. Eng. Jpn.* **1982**, *15*, 342.

(13) Gosman, A. D.; Simitovic, R. An Experimental Study of Confined Jet Mixing. *Chem. Eng. Sci.* **1986**, *41*, 1853.

(14) Perona, J. J.; Hylton, T. D.; Youngblood, E. L.; Cummins, R. L. Jet Mixing of Liquids in Long Horizontal Cylindrical Tanks. *Ind. Eng. Chem. Res.* **1998**, *38*, 1478.

(15) Jayanti, S. Hydrodynamics of Jet Mixing in Vessels. *Chem. Eng. Sci.* **2001**, *56*, 193.

(16) Zughbi, H. D.; Rakib, M. A. Investigations of Mixing in a Fluid Jet Agitated Tank. *Chem. Eng. Commun.* **2002**, *189*, 1038.

(17) Grenville, R. K.; Tilton, J. N. A New Theory Improves the Correlation of Blend Time Data from Turbulent Jet Mixed Vessels. *Trans. Inst. Chem. Eng.* **1996**, *74*, 390.

(18) Grenville, R. K.; Mak, A. T. C.; Ruszkowski, S. Blending of Fluids in Mixing Vessels by Turbulent Recirculating Jets. In *Proceedings of the 1992 IChemE Research Event*; Institution of Chemical Engineers: Rugby, U.K., 1992; p 128.

(19) Ahmad, I. Effects of Geometry and Flow Asymmetry on Mixing in Liquid Jet Agitated Tanks. M.S. Thesis, Department of Chemical Engineering, King Fahd University of Petroleum & Minerals, Dhahran, Kingdom of Saudi Arabia, 2003.

(20) Zughbi, H. D.; Khokhar, Z. H.; Sharma, R. N. Numerical Simulation of Pipeline Mixing with Side and Opposed Tees. *Ind. Eng. Chem. Res.* **2003**, *42*, 5333.

(21) Okita, N.; Oyama, Y. Mixing Characteristics in Jet Mixing. *Jpn. Chem. Eng.* **1963**, *1*, 92.

(22) Van de Vusse, J. G. Vergleichende Rührversuche zum Mischen löslicher Flüssigkeiten in einem 12000 m^3 Behälter, *Chem. Ing. Tech.* **1959**, *31*, 583−587.

Received for review April 24, 2004
Revised manuscript received November 23, 2004
Accepted December 1, 2004

IE0496683